

Experimental Study of the Phase Equilibria in the R-Al-Si Ternary Systems (R: Rare Earth Element) the Ho-Al-Si Isothermal Section at 500°C

Anna Maria Cardinale, Nadia Parodi

Dipartimento di Chimica e Chimica Industriale, Università di Genova, Genova, Italy

Email: cardinal@chimica.unige.it

How to cite this paper: Cardinale, A.M. and Parodi, N. (2019) Experimental Study of the Phase Equilibria in the R-Al-Si Ternary Systems (R: Rare Earth Element) the Ho-Al-Si Isothermal Section at 500°C. *Journal of Materials Science and Chemical Engineering*, 7, 9-17.

<https://doi.org/10.4236/msce.2019.78002>

Received: May 24, 2019

Accepted: August 9, 2019

Published: August 12, 2019

Abstract

The effect of holmium addition to the Al-Si system has been experimentally studied, as the isothermal section at 500°C. The constitution of the alloys has been determined by means of scanning electron microscopy (SEM), electron microprobe analysis (EDXS) and X-ray powder diffraction. The knowledge of the phase relationships in the R-Al-Si ternary systems (R: rare earths element) is essential to deeply understand the technological properties of the Al-Si based alloys, that are useful in different industrial fields. In the system investigated have been identified nineteen ternary fields and twelve two phase fields. Three ternary compounds have been found in this ternary section: τ_2 -Ho₂Al₃Si₂ (mS14-Y₂Al₃Si₂), τ_4 -Ho₂AlSi₂ (oI10-W2CoB₂) and τ_5 -Ho₆Al₃Si (tI80-Tb₆Al₃Si). The results obtained can be useful compared with the other known R-Al-Si systems also for predictive purposes.

Keywords

Al-Si Alloys, Rare Earth, Thermal Analysis

1. Introduction

The Al-Si alloys, both in the as cast and after thermal treatment conditions, have been recognized as interesting materials for the industries (e.g. automotive, heat exchanger, etc.). The addition of a rare earth element, at a very low concentration, can modify the property of the alloys, improving some useful characters as low density and thermal expansion coefficients, good casting performance and weld ability, high wear resistance and temperature strength, good corrosion re-

sistance [1] [2] [3] [4]. All of the above leads to an increasing interest in the study of R-Al-Si based alloys (R being a trivalent rare earth element). The knowledge of the phase equilibria and the transformations that take place during the solidification pathway of foundry aluminum based alloys are crucial, especially in planning and develop new materials. The industrially relevant R-Al-Si alloys have usually a concentration lying near the binary Al-Si eutectic composition and mischmetal (alloy of rare earth metals, whose typical composition includes approximately 50% Ce, 25% La and smaller small amounts of Nd and Pr) is often added.

Moreover, owing to the definition of pseudo-lanthanide [5] it is possible to predict the behavior of an intermetallic phase not prepared yet, when experimental data are available for the adjacent members of this series. Taking into account the aforementioned considerations, investigations of a number of R-Al-Si systems have been carried out by our research group.

2. Literature Data

2.1. Boundary Binary Systems

As far as the binary systems are concerned, the Al-Si phase diagram is a simple eutectic, with the eutectic reaction at 12.2 at % Si and 577 °C and with no intermetallic compounds found in this system [6]. Phase relationships in the Ho-Al system were assessed by [7]. There are five intermetallic compounds: Ho₂Al (oP12-Co₂Si type), Ho₃Al₂ (tP20-Al₂Zr₃ type), HoAl (oP16-ErAl type), HoAl₂ (cF24-MgCu₂ type) and HoAl₃ (hR60-Al₃Ho). The Ho-Si system, was recently assessed by [8]; at 500 °C temperature there are six intermetallic compounds in it as well: Ho₅Si₃ (hP16-Mn₅Si₃ type), Ho₅Si₄ (oP36-Sm₅Ge₄ type), HoSi (oP8-FeB type), Ho₄Si₅, HoSi_{2-b} (hP3-ALB₂ type, ~38 at % Ho) and HoSi_{2-a} (oI12-GdSi₂ type, ~35 at % Ho). The Ho₄Si₅ compound was investigated [9] by means of single crystal X-ray diffraction and its structure was assumed to be Ho₃Si₄oS24-Ho₂Si_{2.67} type.

2.2. R-Al-Si Ternary Systems

To our best effort literature data on R-Al-Si systems isothermal sections (in the whole range of concentrations) and liquid us projections mainly deal with the following: La-Al-Si (0 - 33 at % La) [10], Ce-Al-Si [11], Pr-Al-Si [12] [13], Nd-Al-Si [13], Sm-Al-Si ([13] and refs therein [14]), Eu-Al-Si [15], Gd-Al-Si, Al-Si-Tb and Al-Si-Dy ([13] and refs therein), Ho-Al-Si (0 - 33 at % Ho) [16], Er-Al-Si [17] and Y-Al-Si (0 - 33 at % Y) [18]. In the Ho-Al-Si ternary system, in literature [19], are reported the following compounds: HoAl₂Si₂ hP5-CaAl₂O₂ (τ_1), Ho₂Al₃Si₂ mS14-Y₂Al₃Si₂ (τ_2), HoAlSi oS12-YAlGe (τ_3), Ho₂Al_{1+x}Si_{2-x} oI10-W₂CoB₂ (τ_4) and Ho₆Al₃Si tI80-Tb₆Al₃Si (τ_5).

3. Experimental Techniques

A set of eighteen Ho-Al-Si alloys have been prepared starting from pure ele-

ments (aluminum, silicon and holmium at 99.999, 99.99 and 99.9 mass % purity respectively all supplied by Newmet Koch, Waltham Abbey, England). The starting metals, prepared in little pieces, have been weighed in a proper amount and then arc melted on a water cooled copper plate under vacuum, the samples were re-weighed after melting to check for any mass losses that were always less than 0.5 mass %. The samples have been annealed (in an alumina crucibles sealed in quartz tube under vacuum) at 500°C for 720 hours and then quenched in water.

To characterize the samples after annealing the techniques used have been scanning electron microscopy (SEM), electron probe microanalysis based on energy dispersive X-ray spectroscopy (EDXS) and X-ray diffraction analysis (XRPD). As the metallographic analysis, the samples incorporated in a conductive resin support were prepared according to the standard method by SiC paper and diamond paste polishing. After preparation the samples have been analyzed applying an acceleration voltage of 20 kV for 50 s, and a cobalt standard was used for calibration. For the quantitative analysis the software packaging Inca Energy (Oxford Instruments, Analytical Ltd., Bucks, UK) was employed to process X-ray spectra.

To determine the crystal structures, and calculate lattice parameters of the different phases, the samples were prepared crushing them into powder in an agate mortar; then XRPD analysis was performed by the vertical diffractometer X'Pert MPD (Philips, Almelo, and The Netherlands). The indexing of the obtained diffraction data was achieved by comparison with literature or calculated data (the program Powder Cell [20]), the lattice parameters of the phases were calculated using the program LATCON [21].

4. Results and Discussion

Table 1 reports data obtained from the eighteen samples synthesized and characterized by using SEM/EDXS and X-ray powder diffraction, while **Figure 1** reports the Ho-Al-Si isothermal section at 500°C. It was drawn basing on the experimental data in **Table 1** and contains the samples composition, the field described by means of dotted lines are hypothesized on the basis of the experimental data and the knowledge of the different R-Al-Si systems. In **Figure 2** are shown the micrographic appearance of some selected samples after annealing and quenching, while **Figure 3** reports the PXR pattern of a three phase sample.

4.1. Ternary Isothermal Section

In the present work the system is characterized by nineteen three-phase fields and twelve two-phase fields. According with the previous study of the Ho-Al-Si system [16], the HoAl_2Si_2 (τ_1) compound was not found in the isothermal section at 500°C, this is an unusual behavior when compared with all the other known R-Al-Si systems all showing the tie triangle (Al), (Si) and τ_1 . Furthermore, in the Er-Al-Si isothermal section at 600°C [17] the ErAl_2Si_2 phase was not

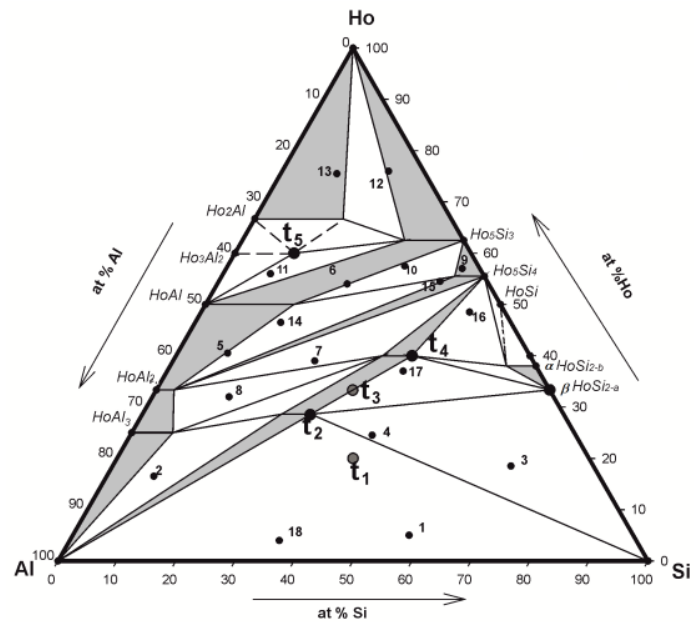


Figure 1. The Ho-Al-Si ternary isothermal section at 500°C, position and code of the samples are superimposed.

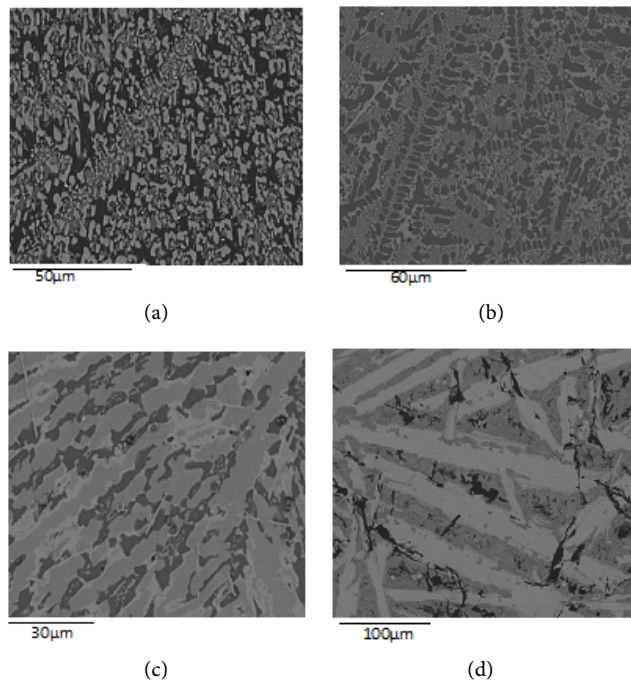


Figure 2. Back scattered electrons (BSE) images of some selected Ho-Al-Si samples after annealing and quenching, the composition is reported in **Table 1**: (a) Sample n.8, primary light $\text{Ho}_2\text{Al}_x\text{Si}_{(2-x)}$ (τ_4), surrounded by small quantity of grey $\text{HoAl}_{(2-x)}\text{Si}_x$ phase plus black $\text{HoAl}_{(3-x)}\text{Si}_x$ compound; (b) Sample n.5, two phase sample constituted by primary dark $\text{HoAl}_{(2-x)}\text{Si}_x$ phase plus light $\text{HoAl}_{(1-x)}\text{Si}_x$ compound; (c) Sample n.14, primary gray $\text{HoAl}_{(1-x)}\text{Si}_x$ crystals surrounded by small quantity of light peritectic $\text{Ho}_5\text{Al}_x\text{Si}_{(4-x)}$ compound plus the black $\text{HoAl}_{(2-x)}\text{Si}_x$ phase; (d) Sample n.16 primary light polygonal crystal of Ho_5Si_4 compound surrounded by peritectic formed Ho_2AlSi_2 (τ_4) and $\text{HoAlSi}_{(2-b)}$ containing 6 at % Al.

Table 1. SEM-EDX and XRPD data on the Ho-Al-Si samples annealed at 500°C and quenched.

N.	Nominal composition Ho, Al, Si/at %	Phases crystal structure	EDXS results Ho, Al, Si/at %	Lattice parameters/nm			
				a	b	c	β °
1	5.0, 38.0, 57.0	Si <i>cF8</i> - <i>C_{diam}</i>	0.0, 0.0, 100.0	0.5428 (1)			
		Al <i>cF4</i> - <i>Cu</i>	0.0, 100.0, 0.0	0.4045 (1)			
		τ_2mS14 - $Y_2Al_3Si_2$	29.0, 45.0, 26.0	1.0083 (2)	0.4013 (1)	0.6560 (8)	100.82
2	16.5, 75.5, 8.0	Al <i>cF4</i> - <i>Cu</i>	0.0, 100.0, 0.0	0.4047 (1)			
		τ_2mS14 - $Y_2Al_3Si_2$	30.0, 45.5, 24.5	1.0091 (9)	0.4015 (5)	0.6572 (9)	100.78
		HoAl _{3-x} Si _x <i>hR60</i> - <i>HoAl₃</i>	26.0, 67.0, 7.0	0.6100 (1)	0.6100 (1)	3.4961 (9)	
3	18.5, 14.0, 67.5	Si <i>cF8</i> - <i>C_{diam}</i>	0.0, 0.0, 100.0	0.5426 (3)			
		τ_2mS14 - $Y_2Al_3Si_2$	29.5, 44.0, 26.5	1.0093 (5)	0.4012 (1)	0.6563 (1)	100.82
		HoSi _{2-a} <i>oI12</i> - <i>GdSi₂</i>	36.0, 0.0, 64.0	0.3915 (2)	0.4015 (1)	1.3371 (9)	
4	25.0, 34.0, 41.0	Si <i>cF8</i> - <i>C_{diam}</i>	0.0, 0.0, 100.0	0.5424 (4)			
		τ_2mS14 - $Y_2Al_3Si_2$	31.0, 43.0, 26.0	1.0090 (7)	0.4011 (3)	0.6561 (5)	100.94
		Ho Al _(2-x) Si _x <i>cF24</i> - <i>MgCu₂</i>	33.0, 64.0, 3.0	0.7825 (2)			
5	40.5, 51.0, 8.5	HoAl _{1-x} Si _x <i>oP16</i> - <i>AlEr</i>	48.0, 40.0, 12.0	0.5900 (2)	1.1401 (9)	0.5578 (3)	
		Ho ₅ Si ₃ <i>hP16</i> - <i>Mn₅Si₃</i>	66.5, 0.0, 33.5	0.8371 (9)	0.8371 (9)	0.6276 (9)	
		HoAl _{1-x} Si _x <i>oP16</i> - <i>AlEr</i>	52.0, 33.0, 15.0	0.5739 (4)	1.1250 (5)	0.5691 (8)	
6	54.0, 24.0, 22.0	Ho ₅ Si ₃ <i>oP36</i> - <i>Ge₄Sm₅</i>	56.0, 0.0, 44.0	0.7335 (4)	1.4406 (5)	0.7614 (2)	
		HoAl _{2-x} Si _x <i>cF24</i> - <i>MgCu₂</i>	33.0, 64.5, 2.5	0.7800 (3)			
		τ_4oI10 <i>W₂CoB₂</i>	43.0, 25.0, 32.0	0.4005 (1)	0.5903 (3)	0.8528 (1)	
7	39.0, 37.0, 24.0	τ_4oI10 <i>W₂CoB₂</i>	42.5, 26.0, 31.5	0.4143 (6)	0.5712 (4)	0.8519 (4)	
		HoAl _{2-x} Si _x <i>cF24</i> - <i>MgCu₂</i>	34.0, 63.0, 3.0	0.7796 (3)			
		HoAl _{3-x} Si _x <i>hR60</i> - <i>HoAl₃</i>	26.5, 68.5, 5.0	0.6011 (6)	0.6011 (6)	3.5550 (5)	
8	32.0, 55.0, 13.0	Ho ₅ Si ₃ <i>hP16</i> - <i>Mn₅Si₃</i>	67.5, 0.0, 32.5	0.8341 (2)	0.8341 (2)	0.6215 (5)	
		Ho ₅ Al _x Si _(4-x) <i>oP36</i> - <i>Ge₄Sm₅</i>	55.0, 4.0, 41.0	0.7315 (6)	1.4429 (6)	0.7610 (2)	
		Ho ₅ Si ₃ <i>hP16</i> - <i>Mn₅Si₃</i>	65.0, 0.0, 35.0	0.8329 (3)	0.8329 (3)	0.6217 (5)	
9	57.0, 3.0, 40.0	Ho ₅ Si _(4-x) Al _x <i>oP36</i> - <i>Ge₄Sm₅</i>	53.5, 6.0, 40.5	0.7321 (5)	1.4439 (1)	0.7616 (9)	
		HoAl _{1-x} Si _x <i>oP16</i> - <i>AlEr</i>	45.0, 41.0, 14.0	0.5752 (4)	1.1167 (2)	0.5579 (6)	
		Ho ₅ Al _x Si _(3-x) <i>hP16</i> - <i>Mn₅Si₃</i>	65.5, 11.5, 23.0	0.8354 (2)	0.8354 (2)	0.6262 (5)	
10	57.5, 12.5, 30.0	HoAl _{1-x} Si _x <i>oP16</i> - <i>AlEr</i>	50.0, 50.0, 0.0	0.5803 (9)	1.1288 (8)	0.5584 (6)	
		τ_5tB80 - <i>Tb₆Al₃Si</i>	55.0, 35.0, 10.0	1.1392 (3)	1.1392 (3)	1.4981 (2)	
		Ho ₅ Al _x Si _(3-x) <i>hP16</i> - <i>Mn₅Si₃</i>	67.5, 8.0, 26.5	0.8355 (3)	0.8355 (3)	0.6266 (5)	
11	76.0, 6.0, 18.0	(Ho) <i>hP2</i> - <i>Mg</i>	100.0, 0.0, 0.0	0.3618 (5)	0.3618 (5)	0.5650 (3)	
		(Ho) <i>hP2</i> - <i>Mg</i>	100.0, 0.0, 0.0	0.3614 (4)	0.3614 (4)	0.5644 (7)	
		Ho ₂ Al _(1-x) Si _x <i>oP12</i> - <i>Co₂Si</i>	66.5, 19.0, 14.5	0.6537 (2)	0.5052 (1)	0.9330 (2)	
12	75.5, 15.0, 9.5	HoAl _{1-x} Si _x <i>oP16</i> - <i>AlEr</i>	52.5, 15.0, 32.5	0.5801 (5)	1.1342 (2)	0.5641 (4)	
		Ho ₅ Al _x Si _(4-x) <i>oP36</i> - <i>Ge₄Sm₅</i>	55.0, 36.5, 8.5	0.7336 (9)	1.4419 (8)	0.7597 (8)	
		HoAl _(2-x) Si _x <i>cF24</i> - <i>MgCu₂</i>	36.5, 60.5, 3.0	0.7815 (1)			
13	46.5, 39.0, 14.5	Ho ₅ Al _x Si _(4-x) <i>oP36</i> - <i>Ge₄Sm₅</i>	55.0, 4.0, 41.0	0.7310 (9)	1.4450 (9)	0.7643 (7)	
		Ho ₅ Si ₄ <i>oP36</i> - <i>Ge₄Sm₅</i>	55.0, 0.0, 45.0	0.7338 (7)	1.4403 (9)	0.7611 (9)	
		τ_4oI10 - <i>W₂CoB₂</i>	42.5, 19.0, 38.5	0.4022 (4)	0.5739 (3)	0.8583 (6)	
14	48.5, 8.5, 45.5	HoSi _{2-b} <i>hP3</i> - <i>AlB₂</i>	38.0, 6.0, 56.0	0.3804 (1)	0.3804 (1)	0.4098 (2)	
		τ_4 - <i>oI10</i> - <i>W₂CoB₂</i>	41.0, 18.0, 41.0	0.4017 (2)	0.5740 (2)	0.8577 (2)	
		τ_2mS14 - $Y_2Al_3Si_2$	29.0, 44.0, 27.0	1.0112 (8)	0.4019 (3)	0.6564 (7)	100.98
15	37.0, 23.0, 40.0	HoSi _{2-a} <i>oI12</i> - <i>GdSi₂</i>	36.0, 0.0, 64.0	0.3929 (4)	0.4019 (2)	1.3348 (8)	
		Si <i>cF8</i> - <i>C_{diam}</i>	0.0, 0.0, 100.0	0.5427 (2)			
		Al <i>cF4</i> - <i>Cu</i>	0.0, 100.0, 0.0	0.4046 (1)			
16	4.0, 60.5, 35.5	τ_2mS14 - $Y_2Al_3Si_2$	29.5, 44.0, 26.5	1.0083 (5)	0.4013 (2)	0.6560 (4)	100.81

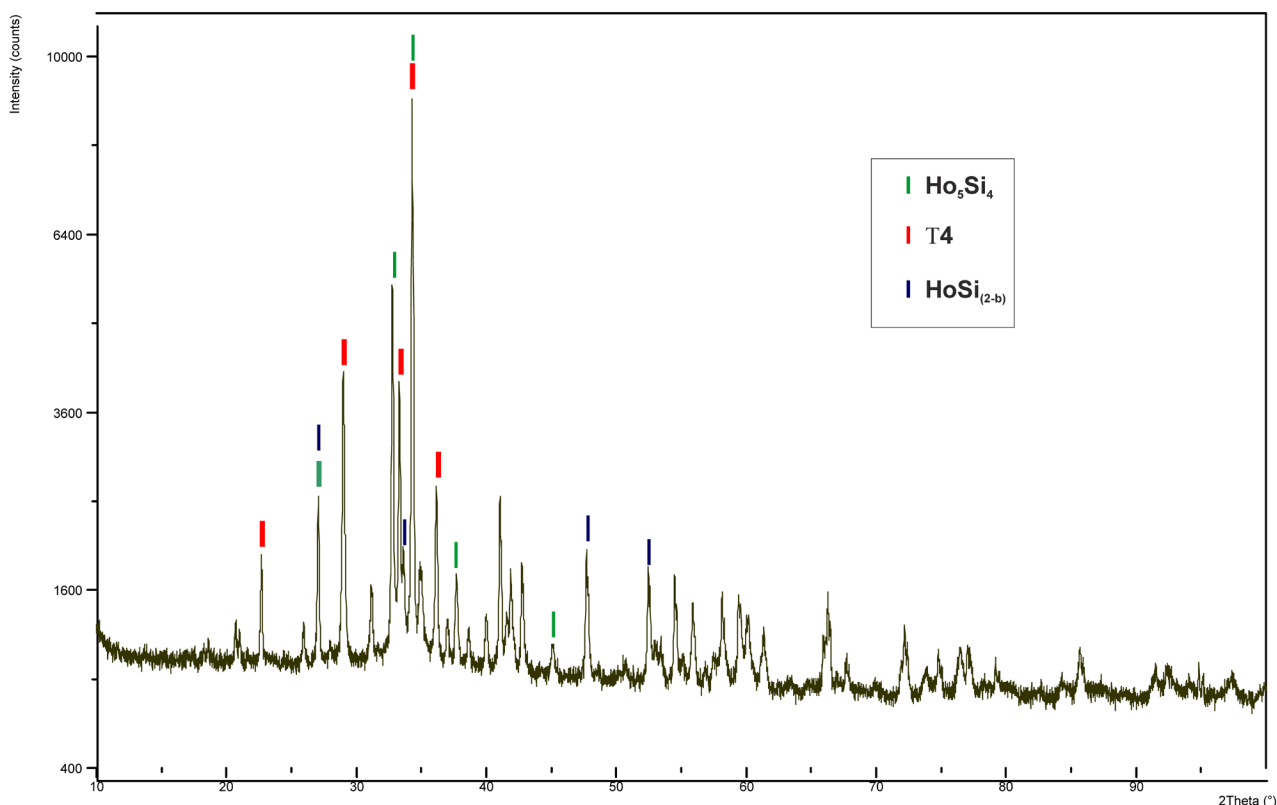


Figure 3. X-ray powder pattern of sample n.16 (see **Table 1**).

found and the tie triangle in the Al and Si rich part of the system shows the same vertices as the Ho-Al-Si system. The micrographs of four representative samples are reported in **Figure 2**. **Figure 2(a)** shows the appearance of the sample n.8 that describes the triangle constituted by the two phases $\text{HoAl}_{(2-x)}\text{Si}_x$ and $\text{HoAl}_{(3-x)}\text{Si}_x$ (respectively grey and black and both at their maximum silicon solubility), plus light $\text{Ho}_2\text{Al}_x\text{Si}_{(2-x)}$ (τ_4) at its maximum aluminum solubility value. In **Figure 2(b)**, the sample n.5, pertaining to the two $\text{HoAl}_{(2-x)}\text{Si}_x$ and $\text{HoAl}_{(1-x)}\text{Si}_x$ phase field, shows dark primary $\text{HoAl}_{(2-x)}\text{Si}_x$ crystals and the binary eutectic between the primary phase and $\text{HoAl}_{(1-x)}\text{Si}_x$ compound, the medium eutectic composition is Ho 42 at % and Al 46 at % very close to the composition of the sample as confirmed by the micrographic feature. Ongoing throughout the system to the Ho richest part, in **Figure 2(c)** the sample n.14 is a three phase sample with gray primary $\text{HoAl}_{(1-x)}\text{Si}_x$ compound (at its maximum silicon solubility) surrounded by a small quantity of light $\text{Ho}_5\text{Al}_x\text{Si}_{(4-x)}$ of peritectic formation, plus black $\text{HoAl}_{(2-x)}\text{Si}_x$ phase. The sample n.16, in **Figure 2(d)** belongs to the $\text{Ho}_2\text{Al}_x\text{Si}_{(2-x)}$ (τ_4), Ho_5Si_4 and HoSi_{2-b} tie triangle; the PXRD pattern of sample n.16 is reported in **Figure 3**, the main reflections of the three phases identify are highlighted.

4.2. Ternary Compounds

Five ternary intermetallic compounds, are reported in literature: τ_1 - HoAl_2Si_2 (hP5-CaAl₂Si₂), τ_2 - $\text{Ho}_2\text{Al}_3\text{Si}_2$ (mS14-Y₂Al₃Si₂), τ_3 - HoAlSi (oS12-YAlGe), τ_4 - Ho_2AlSi_2

(oI10-W2CoB₂) and τ_5 -Ho₆Al₃Si (tI80-Tb₆Al₃Si). In this work only three compounds were identified at 500°C; the τ_3 structure seems not to form in the system at 500°C and the τ_1 phase was not found in the system as discussed in the previous section. The τ_2 compound shows a homogeneity range with constant Ho content, dissolving up to 45 at % Al (stoichiometric composition is located at 42.8 at % Al). As the τ_4 compound has been proved the substitution with Al for Si in a range from 20.0 at % Al (stoichiometric composition) to 25 at % Al.

4.3. Binary Compounds

As expected different boundary binary compounds entry the ternary system, the homogeneity ranges minor of 2 at % are not taking into account. For each compound involved the solubility limit of the third element has been assumed as the medium value of the different experimental measurements in the different samples investigated. From the Ho-Al system, the HoAl₃, HoAl₂ and HoAl compounds dissolve respectively 7 at %, 3 at % and 15 at % silicon. Ongoing from the Si to the Ho richest part of the binary Ho-Si phase diagram some compounds dissolve aluminium in the following percentage: HoSi₂₋₃ 4 at %, Ho₅Si₄ 5 at % and Ho₅Si₃ 10 at %.

5. Conclusions

The Ho-Al-Si-isothermal section at 500°C has been studied in the whole composition range, as the phase relationships the main conclusions are the following:

- The studied system consists of nineteen three-phase fields and twelve two-phase fields.
- Of the five known ternary compounds only τ_2 -Ho₂Al₃Si₂ (mS14-Y₂Al₃Si₂), τ_4 -Ho₂AlSi₂ (oI10-W2CoB₂) and τ_5 -Ho₆Al₃Si (tI80-Tb₆Al₃Si) have been found in the system at 500°C, according with [16]. The τ_2 and τ_4 phases dissolve aluminum up to 45 at % and 25 at % respectively.
- Different binary compounds dissolve the third element extending into the ternary system.
- By comparing the different known ternary isothermal sections, some points can be highlighted. All the sections are characterized by the presence of intermediate phases with R content up to 60 at % rare earth. The number of phases decreases on going from the light (Pr, Nd, Sm) to the heavy rare earths (Gd, Tb, Dy, Er). Only the RAl₂Si₂ compounds form along the whole lanthanides series as point compounds; nevertheless in the previously studied Ho-Al-Si [16] and Er-Al-Si [17] isothermal sections this compound has not been founded. From La to Dy at low R content the three-phase equilibrium: (Al)/(Si)/RAl₂Si₂ occurs. Many R-Si and R-Al compounds extend in the ternary system forming solid solutions at a constant R-content.

Conflicts of Interest

The authors declare no conflicts of interest regarding the publication of this paper.

References

- [1] Slattery, B.E., Perry, T. and Edrissy, A. (2009) Microstructural Evolution of a Eutectic Al-Si Engine Subjected to Severe Running Conditions. *Mat. Sci. and Eng. A*, **512**, 76-81. <https://doi.org/10.1016/j.msea.2009.01.025>
- [2] Miller, W.S., Zhuang, L., Bottema, J., Wittebrood, A.J., De Smet, P., Haszler, A. and Vieregge, A. (2000) Recent Development in Aluminum Alloys for the Automotive Industry. *Mat. Sci. and Eng. A*, **280**, 37-49. [https://doi.org/10.1016/S0921-5093\(99\)00653-X](https://doi.org/10.1016/S0921-5093(99)00653-X)
- [3] Zhu, M., Jian, Z., Yao, L., Liu, C., Yang, G. and Zhou, Y. (2011) Effect of Mischmetal Modification Treatment on the Microstructure, Tensile Properties, and Fracture Behavior of Al-7.0%Si-0.3%Mg Foundry Aluminum Alloys. *J Mater. Sci*, **46**, 2685-2694. <https://doi.org/10.1007/s10853-010-5135-7>
- [4] Cardinale, A.M., Macciò, D., Luciano, G., Canepa, E. and Traverso, P. (2016) Thermal and Corrosion Behavior of as Cast Al-Si Alloys with Rare Earth. *J. Alloys Compd*. <https://doi.org/10.1016/j.jallcom.2016.11.066>
- [5] Gschneidner Jr., K.A. (1980) The Rare Earths in Modern Science and Technology. In: McCarthy, G.J., Rhine, J.J. and Silber, H.B., Eds., Plenum, New York, 2, 13-23.
- [6] Murray, J.L. and McAlister, A.J. (1984) The Al-Si (Aluminum-Silicon) System. *Bull. of Alloy Phase Diagrams*, **5**, 74-84. <https://doi.org/10.1007/BF02868729>
- [7] Jin, L., Kang, Y.-B., Chartrand, P. and Fuerst, C.D. (2010) Thermodynamic Evaluation and Optimization of Al-Gd, Al-Tb, Al-Dy, Al-Ho and Al-Er Systems Using a Modified Quasichemical Model for the Liquid. *CALPHAD*, **34**, 456-466. <https://doi.org/10.1016/j.calphad.2010.08.004>
- [8] Kim, J. and Jung, I.H. (2015) Critical Evaluation and Thermodynamic Optimization of the Si-RE Systems: Part II. Si-RE System (RE= Gd, Tb, Dy, Ho, Er, Tm, Lu and Y). *J. Chem. Thermodynamics*, **81**, 273-297. <https://doi.org/10.1016/j.jct.2014.08.014>
- [9] Ijjaali, I., Venturini, G. and Malaman, B. (1998) X-Ray Single Crystal Refinement of the Ho₃Si₄ Structure. *J. Alloys Compd*, **269**, L6-L8. [https://doi.org/10.1016/S0925-8388\(97\)00626-9](https://doi.org/10.1016/S0925-8388(97)00626-9)
- [10] Murav'eva, A.O. (1971) The Systems La-Al-Si and La-Al-Sb in the Region 0-33.3 at % La. *Vestn. Lviv Univ. Ser. Khim*, **12**, 8-9.
- [11] Li, Y., Li, Z., Liu, Y., Wang, X., Zhao, M. and Yin, F. (2014) Isothermal Section of Al-Si-Ce Ternary System at 1073 K. *J. of Phase Equil. and Diffusion*, **35**, 276-283. <https://doi.org/10.1007/s11669-014-0306-x>
- [12] Cardinale, A.M., Macciò, D. and Saccone, A. (2015) Phase Relationships of the R-Al-Si Systems: The Pr-Al-Si Isothermal Section at 500°C. *J. Therm. Anal. And Calorim*, **121**, 1151-1157. <https://doi.org/10.1007/s10973-015-4906-4>
- [13] Cardinale, A.M. and Parodi, N. (n.d.) R-Al-Si Systems (R: Pr, Nd): Experimental Investigation of Phase Equilibria in the Al-Rich Corner.
- [14] Markoli, B., Spaic, S. and Zupanic, F. (2001) The Constitution of Alloys in the Al-Rich Corner of the Al-Si-Sm Ternary System. *Z. Metallkde*, **92**, 1098-1102.
- [15] Zarechnyuk, O.S. and Yanson, T.I. (1982) The Eu-Al-Si System within a Range of 0 - 33.3 Atomic Parts of Europium. *Akad. NaukUkr. RSR*, **4**, 30-31.
- [16] Zhuang, Y.H., Li, J.Q. and Zeng, L.M. (1990) The Isothermal Section (500°C) of the Phase Diagram of the Al-Ho-Si Ternary System. *J. Less-Common Met*, **157**, 47-53. [https://doi.org/10.1016/0022-5088\(90\)90405-9](https://doi.org/10.1016/0022-5088(90)90405-9)

- [17] Pukas, S., Lasocha, W. and Gladyshevskii, R. (2009) Phase Equilibria in the Er-Al-Si System at 873 K. *CALPHAD*, **33**, 23-26.
<https://doi.org/10.1016/j.calphad.2008.07.017>
- [18] Murav'eva, A.O., Zarechnyuk, O.S. and Gladyshevskii, E.I. (1971) The system-sy-Al-Si(Ge, Sb) in the Range 0 - 33.3 at % Y. *Izv. Akad. Nauk SSSR Neorg. Mater*, **1**, 38.
- [19] Villars, P. and Cenzual, K. (n.d.) Pearson's Crystal Data-Crystal Structure Database for Inorganic Compounds (on DVD), Release 2017/18, ASM International, Materials Park, Ohio, USA.
- [20] Kraus, W. and Nolze, G. (1999) Powder Cell for Windows, Berlin.
- [21] King, G. and Schwarzenbach Latcon, D. (2000) Xtal3.7 System. In: Hall, S.R., du Boilay, D.J. and Olthof-Hazekamp, R., Eds., University of Western, Australia.